

[EN-028] On the use of MIMO in aeronautical communications

⁺ B. Holter J. E. Håkegård T. A. Myrvoll

Department of Communication Systems

SINTEF ICT

Trondheim, Norway

[bengt.holter|jan.e.hakegard|torandre.myrvoll]@sindef.no

Abstract In this paper, it is shown that it is possible to use multiple-input multiple-output (MIMO) spatial multiplexing systems in aeronautical communications over an extended range even in the presence of a strong line-of-sight (LOS) component. Results originally derived to maximize the MIMO capacity in fixed range applications dominated by a LOS component is exploited to show that a high rank channel matrix may not only be offered for a fixed distance but can be maintained over an extended range and area in a MIMO ground-to-air communication system with $n_T = 2$ transmit antennas (ground terminal) and $n_R \geq 2$ receive antennas (aircraft). Numerical results are presented for an $n_R \times n_T$ MIMO system in a Ricean fading channel assuming communication between a ground terminal and an aircraft in the en-route domain.

Keywords MIMO, Aeronautical communications, Chebyshev polynomials

1. INTRODUCTION

The introduction of multiple-input multiple-output (MIMO) systems has contributed to vast improvements in capacity and reliability in wireless communications. MIMO systems thrive in rich multipath environments, since it leads to antenna decorrelation and a high rank channel matrix.¹ In these conditions, a MIMO system can offer a linear increase in capacity that is proportional to the minimum number of transmit and receive antennas. As a result, the majority of research on MIMO communications have been focused on systems operating in a rich multipath environment.

MIMO signalling techniques are currently been considered for future aeronautical communication systems within Europe and the United States. In particular, the future airport datalink system AeroMACS will be based on IEEE802.16 technology involving MIMO, and aeronautical satellite communications consider introducing MIMO techniques for use in high latitudes and for low satellite elevation angles.

A more theoretical approach to improve the performance of future aeronautical communication systems by increasing the capacity and reliability in air-to-ground links has been proposed in [1]. Aeronautical channels are typically Ricean fading channels, characterized by the presence of a strong line-of-sight (LOS) component. A LOS component will usually reduce the performance of a MIMO system, since there is a large probability that all the signals will be conveyed through the same channel. Effectively, it means that the MIMO channel matrix in a LOS environment becomes rank-deficient (not full rank). This reduces

the spatial multiplexing gain of the system since several data streams can be separated by an equalizer only if the fading processes of the spatial channels are (nearly) independent.

A possible solution to this challenge was indicated in [2], stating that a linear increase in capacity could be achieved by increasing the distance between the antennas at the transmitter to produce antenna patterns with nulls on all but one receiver antenna. By this approach, independent channels on the same carrier frequency could be established. A similar technique was indicated in [3, Sec. III].

Motivated by the results in [2] and [3], the authors in [4] and [5] propose a design methodology to achieve a full-rank MIMO channel matrix in a LOS environment. It is shown that orthogonality between subchannels of the channel matrix can be related to the product of the inter-element spacings of the antennas at the transmitter and receiver, assuming uniform linear array (ULA) antennas at both ends. They both introduce more general geometrical models than that applied in earlier works to gain additional insight, in particular to quantify a reduction from optimal performance caused by misalignment between the transmitter and receiver antenna arrays. In [4], the performance is evaluated with respect to both ergodic and outage capacity using a Ricean fading channel model. The results show that even with some deviations from an optimal design, a LOS MIMO system may outperform a system operating on independent and identically distributed (i.i.d.) Rayleigh fading channels in terms of Shannon capacity.

¹In some cases, the channel matrix may still be of rank one even though the antennas at both ends are uncorrelated. Such a MIMO channel is commonly called a "pinhole" channel.

The results presented in [4] and [5] have contributed to create new interest in the use of spatial multiplexing in environments with a strong LOS component. Notably, results have been presented in recent publications on fixed wireless access schemes [6], indoor communication [7], and vehicle-to-roadside communication [8]. However, to the author's knowledge, no one has yet looked into the use of the results for aeronautical communications. Hence, in this paper, the theoretical results in [4] are re-visited but viewed from an aeronautical perspective, where the range now is variable rather than fixed. Note however that the particular view of a variable range is not original to this paper, since it has been addressed to some extent in small range applications [7–9]. In particular, it is shown in [7] that a MIMO system operating in a LOS environment may be used over a larger set of ranges by using optimized nonuniform antenna arrays rather than uniform antenna arrays.

In this paper, a MIMO system which involves a ground terminal with 2 antennas and a ULA antenna mounted on the aircraft wings is proposed. The channel capacity of such a system is quantified and presented as a function of range and angle between the ground antenna array and the aircraft antenna array. Numerical results show that the channel matrix may be kept at full rank in a LOS environment over an extended range, which is essential to accommodate MIMO communication in the en-route domain.

The paper is organized as follows. In Section 2, the system and channel model is presented. Then, for clarity, information theoretic results on the channel capacity of a MIMO system are reviewed in Section 3. In Section 4, numerical and analytical results that quantify the performance of a MIMO system operating in a LOS environment are presented. The conclusions of the paper are presented in Section 5.

2. CHANNEL MODEL

Using complex baseband vector notation, the input/output relations of a narrowband single user MIMO link with n_T transmit antennas and n_R receive antennas can be written as

$$\mathbf{y} = \sqrt{\Omega}\mathbf{H}\mathbf{x} + \mathbf{n}, \quad (1)$$

where $\mathbf{y} \in \mathbb{C}^{n_R \times 1}$ is the received signal vector, $\mathbf{x} \in \mathbb{C}^{n_T \times 1}$ is the transmitted signal vector, $\mathbf{H} \in \mathbb{C}^{n_R \times n_T}$ is the channel matrix, Ω is the common power attenuation factor for all the channels in the channel matrix, and $\mathbf{n} \in \mathbb{C}^{n_R \times 1}$ is an additive noise vector containing i.i.d. circularly symmetric Gaussian elements with zero mean and variance σ^2 (in short $CN(0, \sigma^2)$).² As in [10], \mathbf{H} represents a *normalized* channel matrix, which means that all entries of the matrix have unit

²A circularly symmetric complex Gaussian random variable with zero mean and variance σ^2 is a complex random variable $x + jy$, where x and y are independent and normally distributed with zero mean and variance $\sigma^2/2$.

average power. The path loss for all subchannels is accounted for by the common parameter Ω . This normalization is convenient since it makes the average signal-to-noise ratio (SNR) independent of \mathbf{H} .

A general entry in \mathbf{H} is denoted $h_{m+1,n+1}$, representing the complex channel gain between transmit antenna $n \in \{0, 1, \dots, n_T - 1\}$ and receive antenna $m \in \{0, 1, \dots, n_R - 1\}$. The channel matrix may then be written as

$$\mathbf{H} = \begin{bmatrix} h_{1,1} & h_{1,2} & \dots & h_{1,n_T} \\ h_{2,1} & h_{2,2} & \dots & h_{2,n_T} \\ \vdots & \vdots & \ddots & \vdots \\ h_{n_R,1} & h_{n_R,2} & \dots & h_{n_R,n_T} \end{bmatrix}. \quad (2)$$

For simplicity (and later reference), it can also be presented in terms of its individual column vectors \mathbf{h}_n as

$$\mathbf{H} = \begin{bmatrix} | & | & \dots & | \\ \mathbf{h}_0 & \mathbf{h}_1 & \dots & \mathbf{h}_{n_T-1} \\ | & | & \dots & | \end{bmatrix}. \quad (3)$$

In the en-route domain, the aeronautical channel is commonly characterized as a fast fading (rapidly time varying) channel where the amplitude of the received signal follows a Rice distribution [11]. In this case, the MIMO channel matrix in (2) may be written as a sum of two parts, a deterministic part (LOS component) and a Rayleigh fading part (Non-LOS (NLOS) component):

$$\mathbf{H} = a\mathbf{H}_{\text{LOS}} + b\mathbf{H}_{\text{NLOS}}. \quad (4)$$

The power ratio of the two matrix components defines the Rice factor as $K = a^2/b^2$, which commonly is expressed in decibels as $K = 10 \log_{10} \left(\frac{a^2}{b^2} \right)$ dB. In the following, it is assumed that the sum power of the components is normalized, i.e. $a^2 + b^2 = 1$. With this assumption, a and b can be expressed in terms of the Rice factor as $a = \sqrt{K/(K+1)}$ and $b = \sqrt{1/(K+1)}$.

For simplicity, a flat fading channel is assumed, which means that the channel impulse response of each subchannel in the channel matrix consists of one tap only (thus no inter-symbol interference). In addition, since the channel capacity subsequently is used as a measure to quantify the performance, coherent detection with perfect channel knowledge at the receiver is assumed throughout the paper. In practice, perfect channel knowledge is not possible in a rapidly time varying channel, so the results of this paper will only serve as performance upper bounds.³

³In [12], performance degradation of basic modulation schemes in a rapidly time varying channel using a first order autoregressive channel model is presented.

2.1. LOS channel

The matrix \mathbf{H}_{LOS} represents the transfer function for signals that have traveled from the transmitter to the receiver by a direct path. As a result, it is a deterministic matrix since all the entries only depend on the distance between the transmit and receive antenna elements. The entries of \mathbf{H}_{LOS} can then in general be expressed as

$$h_{m+1,n+1} = \exp(j\beta r_{mn}), \quad (5)$$

where $\beta = 2\pi/\lambda$ is the wave number, λ is the wavelength of the transmitted signal, and r_{mn} is the direct path length between transmit antenna n and receive antenna m . In this paper, the expression for r_{mn} is identical to [4, Eq. (7)], which is based on the geometrical model depicted in Fig.1. It shows a general MIMO system with ULA antennas at both ends of the link. This means that the inter-element distance between adjacent antennas in each of the arrays is fixed. The antenna inter-element distance at the transmitter and receiver are denoted d_t and d_r , respectively. With n_T transmit antennas and n_R receive antennas, the total length of the transmitter array becomes $(n_T - 1)d_t$, while the length of the receiver array becomes $(n_R - 1)d_r$. The distance (or range) between the transmitter and receiver is denoted R , and it is defined to be the distance between the lower end of the two arrays. Finally, the ULAs are not restricted to be parallel, and the angles θ_t , θ_r , and ϕ_r are used to model the impact of arbitrary orientations. Based on the geometry in Fig.1, the distance r_{mn} in (5) can be expressed as [4, Eq. (7)]

$$\begin{aligned} r_{mn} &\approx R + md_r \sin \theta_t \cos \phi_r - nd_t \sin \theta_t \\ &+ \frac{(md_r \sin \theta_r \sin \phi_r)^2}{2R} \\ &+ \frac{(md_r \cos \theta_r - nd_t \cos \theta_t)^2}{2R}. \end{aligned} \quad (6)$$

The approximation sign in (6) is used as a reminder that the result is valid only when R is much larger than the transmit and receive antenna dimensions.

2.2. NLOS channel

The matrix \mathbf{H}_{NLOS} represents the transfer function for signals that are received as a result of reflection, diffraction and scattering from the environment. The combined reception of such signals are commonly modeled by a stochastic process. As in [10], the entries of \mathbf{H}_{NLOS} are modeled as circular symmetric complex Gaussian random variables with zero mean and variance σ_h^2 . Hence,

$$h_{m+1,n+1} \sim \mathcal{CN}(0, \sigma_h^2). \quad (7)$$

Since the individual channel gains in this case will be Rayleigh distributed, \mathbf{H}_{NLOS} is commonly referred to as a Rayleigh fading matrix. To keep the matrix

normalized, it is assumed that $\sigma_h^2 = 1$. Since the aeronautical channel is a rapidly time varying channel, it is assumed that \mathbf{H}_{NLOS} is memoryless, i.e. for each use of the channel and independent realization of \mathbf{H}_{NLOS} is drawn.

3. CHANNEL CAPACITY

The channel capacity is a measure of the amount of information which can be transmitted and received with a negligible probability or error. With a uniform power distribution among the transmit antennas, the channel capacity of a MIMO system is equal to

$$C = \log_2 \left[\det \left(\mathbf{I}_M + \frac{\bar{\gamma}}{n_T} \mathbf{W} \right) \right] \text{ bit/s/Hz}, \quad (8)$$

where $M = \min\{n_R, n_T\}$, \mathbf{I}_M is the $M \times M$ identity matrix, $\bar{\gamma} = \frac{\Omega P_T}{\sigma^2}$ is the average received SNR, P_T is the total average transmit power,⁴ and

$$\mathbf{W} = \begin{cases} \mathbf{H}\mathbf{H}^H, & n_R < n_T \\ \mathbf{H}^H\mathbf{H}, & n_R \geq n_T \end{cases} \quad (9)$$

is the channel covariance matrix. The superscript H in (9) denotes Hermitian transpose. Note that (8) is valid only for a given channel realization. When \mathbf{H} is stochastic, C becomes a random variable and the *ergodic* channel capacity (mean capacity over all channel realizations for a given average SNR) can be obtained as $\bar{C} = E_H(C)$.⁵

Using the matrix notation introduced in (3) and assuming $n_R \geq n_T$, the covariance matrix \mathbf{W} can be expressed as

$$\mathbf{W} = \begin{bmatrix} \mathbf{h}_0^H \mathbf{h}_0 & \mathbf{h}_0^H \mathbf{h}_1 & \dots & \mathbf{h}_0^H \mathbf{h}_{n_T-1} \\ \mathbf{h}_1^H \mathbf{h}_0 & \mathbf{h}_1^H \mathbf{h}_1 & \dots & \mathbf{h}_1^H \mathbf{h}_{n_T-1} \\ \vdots & \vdots & \ddots & \vdots \\ \mathbf{h}_{n_T-1}^H \mathbf{h}_0 & \mathbf{h}_{n_T-1}^H \mathbf{h}_1 & \dots & \mathbf{h}_{n_T-1}^H \mathbf{h}_{n_T-1} \end{bmatrix}. \quad (10)$$

Using eigenvalue decomposition on \mathbf{W} , (8) may alternatively be written as [14]

$$\begin{aligned} C &= \sum_{i=1}^{r_\omega} \log_2 \left(1 + \frac{\bar{\gamma}}{n_T} \omega_i \right), \\ &= \log_2 \left(\prod_{i=1}^{r_\omega} \left(1 + \frac{\bar{\gamma}}{n_T} \omega_i \right) \right), \end{aligned} \quad (11)$$

where $\{\omega_i\}_{i=1}^M$ are the eigenvalues of \mathbf{W} , and $r_\omega \leq M$ is the rank of \mathbf{W} (or \mathbf{H}).

⁴For a pure Rayleigh fading channel, a uniform power distribution is optimal in the sense that it maximizes the capacity, but this is generally not the case for a Ricean fading channel. However, a uniform power distribution is asymptotically optimal as the SNR tends to infinity if $n_R \geq n_T$ [13].

⁵ $E_H(\cdot)$ denotes the expectation over all channel realizations.

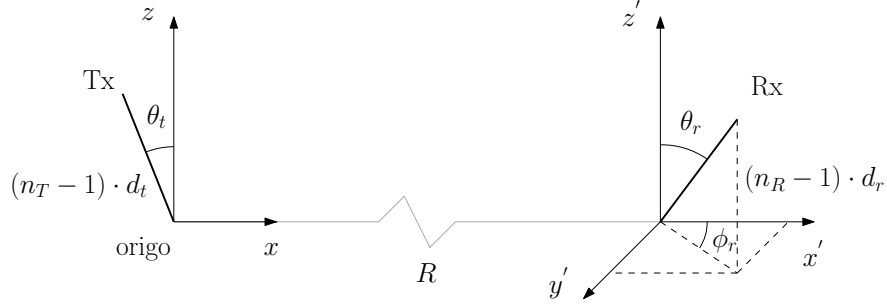


Figure 1 A general MIMO system with uniform linear arrays at both the transmitter and the receiver [4, Fig. 1].

Table 1 List of the eight first Chebyshev polynomials of the second kind.

n_R	$U_{n_R-1}(\cos x)$
1	1
2	$2 \cos x$
3	$4 \cos^2 x - 1$
4	$8 \cos^3 x - 4 \cos x$
5	$16 \cos^4 x - 12 \cos^2 x + 1$
6	$32 \cos^5 x - 32 \cos^3 x + 6 \cos x$
7	$64 \cos^6 x - 80 \cos^4 x + 24 \cos^2 x - 1$
8	$128 \cos^7 x - 192 \cos^5 x + 80 \cos^3 x - 8 \cos x$

In the following, it will be focused on the matrix \mathbf{H}_{LOS} since the overall rank of \mathbf{H} in a strong LOS environment in general will be dominated by the rank of \mathbf{H}_{LOS} . As such, it is convenient to define the associated LOS version of (9) as $K \rightarrow \infty$ (pure LOS channel). In this case, the channel covariance matrix can be defined as

$$\mathbf{M} = \begin{cases} \mathbf{H}_{\text{LOS}} \mathbf{H}_{\text{LOS}}^H, & n_R < n_T \\ \mathbf{H}_{\text{LOS}}^H \mathbf{H}_{\text{LOS}}, & n_R \geq n_T \end{cases}. \quad (12)$$

The capacity may then be expressed as

$$C = \log_2 \left(\prod_{i=1}^{r_\lambda} \left(1 + \frac{\bar{\gamma}}{n_T} \lambda_i \right) \right), \quad (13)$$

where $\{\lambda_i\}_{i=1}^M$ are the eigenvalues of \mathbf{M} , and $r_\lambda \leq M$ is the rank of \mathbf{M} (or \mathbf{H}_{LOS}).

From (13), it is observed that the rank of \mathbf{M} plays an important part in maximizing the capacity of a MIMO system. A MIMO system thrives in a rich multipath environment since it contributes to realize a high rank channel matrix. However, when a strong LOS component is present, \mathbf{H}_{LOS} becomes rank deficient since all the signals then are conveyed through the same

channel. Hence, in order to exploit MIMO spatial multiplexing techniques in a LOS channel, methods that can contribute to increase the rank of \mathbf{M} must be employed. Note that the rank of a matrix usually is defined as the number of non-zero singular values. However, when the rank of \mathbf{M} is maximized, the rank of \mathbf{H}_{LOS} is also maximized since the squared singular values of \mathbf{H}_{LOS} are equal to the eigenvalues of \mathbf{M} . As mentioned in the introduction, the authors in [4] and [5] have proposed a design methodology to achieve a full rank MIMO channel matrix in a LOS environment. With the assumption of ULA antennas at both ends, the technique is to use an optimized inter-element distance at both the transmitter and the receiver to obtain a full rank channel matrix at a given fixed range R . In [4], the key design parameter is presented as the product of d_t and d_r , referred to as the *antenna separation product* (ASP). The optimal ASP which maximizes (13) for a pure LOS channel is equal to [4, Eq. (12)]

$$d_t d_r = \frac{\lambda R}{N \cos \theta_t \cos \theta_r}, \quad (14)$$

where $N = \max(n_R, n_T)$. When the ASP is equal to (14), the rank of \mathbf{M} (and \mathbf{H}_{LOS}) is maximized and equal to $r_\lambda = M$.

In the following, a MIMO system with $n_T = 2$ and $n_R \geq n_T$ will be assumed. In this case, the maximum rank of \mathbf{M} (or \mathbf{H}_{LOS}) is $r_\lambda = 2$. The eigenvalues of \mathbf{M} for a $n_R \times 2$ MIMO system can then be expressed compactly as (see Appendix)

$$\lambda_1 = n_R + U_{n_R-1}(\cos x), \quad (15)$$

$$\lambda_2 = n_R - U_{n_R-1}(\cos x), \quad (16)$$

where $x = \frac{\pi}{n_R \eta}$, $\eta = \frac{\lambda R}{N \cos \theta_t \cos \theta_r d_t d_r}$, and $U_{n_R-1}(\cdot)$ is a Chebyshev polynomial of the second kind. The eight first Chebyshev polynomials of the second kind as a function of n_R are listed in Table 1.

The symbol η is called the *deviation factor*, and it is defined in [4, Eq. (13)] as the ratio between the optimal ASP in (14) (in the following denoted ASP_{opt}) and the actual ASP, i.e.

$$\eta = \frac{ASP_{opt}}{ASP} = \frac{\lambda R}{N \cos \theta_t \cos \theta_r d_t d_r}. \quad (17)$$

In [4], η is used as a measure (in dB) for how far the actual ASP is from the optimal ASP for a fixed range R . Hence, if $\eta > 1$, the actual ASP is too small compared to the optimal value in (14). If $\eta < 1$, the actual ASP is too large. However, once the optimal d_t and d_r have been established for a fixed range denoted R_{opt} , deviations from R_{opt} will cause η to deviate from its optimal value of one as well. Hence, in this paper, $\eta > 1$ is used to signify a system that operates at $R > R_{opt}$. Similarly, $\eta < 1$ signifies a system that operates at $R < R_{opt}$. As such, η is in this paper used as a measure for the performance of a MIMO system as the range deviates from its optimal fixed value.

Finally, ρ is defined as the normalized correlation coefficient between the receive array responses from the l th and k th transmit element ($l, k \in [0, 1]$)

$$\rho \triangleq \frac{|\mathbf{h}_l^H \mathbf{h}_k|}{\|\mathbf{h}_l\| \cdot \|\mathbf{h}_k\|} = \frac{|U_{n_R-1}(\cos x)|}{n_R}. \quad (18)$$

With the aid of (15), (16) and (18), the capacity in (13) for an $n_R \times 2$ MIMO system can then be expressed compactly in closed form as

$$C = \log_2 \left(1 + \bar{\gamma} n_R + \left(\frac{\bar{\gamma} n_R}{2} \right)^2 (1 - \rho^2) \right). \quad (19)$$

For $n_R = 2$, (19) reduces to [15, Eq. 20].

4. GROUND-TO-AIR COMMUNICATION

This section is divided into two parts. In the first part, numerical and analytical results of a ground-to-air MIMO communication system are presented for a pure LOS channel, i.e. for \mathbf{H}_{LOS} only. In the second part, similar results are presented for the complete channel matrix \mathbf{H} , which is a stochastic channel. The numerical results in the second part are therefore obtained by averaging over many channels realizations. In both parts, it is assumed that the transmitter (ground terminal) is equipped with $n_T = 2$ antennas and the receiver (aircraft) is equipped with $n_R \geq 2$ antennas. The distance between the two ground terminal antennas is denoted d_t , whereas the aircraft antenna array is assumed to be an ULA with inter-element

distance d_r . In the aircraft, the antennas are assumed to be conformal antennas evenly distributed along the aircraft wings.

For a given channel realization and a fixed number of antennas, the capacity is a function of the SNR. The SNR is again a function of the range, since the signal level naturally decreases as a function of range which then effectively also reduces the SNR. However, in all the numerical results presented in this paper, the SNR is kept fixed as a function of range in order to isolate the impact of the range from the impact of the SNR. Otherwise, it would be difficult to know whether a change in the capacity is caused by a change in the range or by a change in the SNR if they both vary at the same time. Hence, to better visualize the impact of a variable range on the capacity of the system, the SNR is kept fixed as a function of range.

4.1. Part 1 - Deterministic channel

4.1.1. 2×2

As a reference, the capacity of a 2×2 MIMO system is used. In Fig.2, (19) is depicted as a function of R when d_t and d_r are selected to maximize the capacity at $R_{opt} = 150$ km. In order to maximize the capacity at such a long range, either d_t , d_r or both must be quite large. For this reason, the inter-element distance at the ground terminal is in this paper selected to be fixed at $d_t = 1500$ m. This makes it possible to maximize the capacity using a comparatively small inter-element distance in the aircraft, which is assumed to be a commercial passenger jet. With $d_t = 1500$ m, the capacity is maximized at $R_{opt} = 150$ km with $d_r = 15$ m.

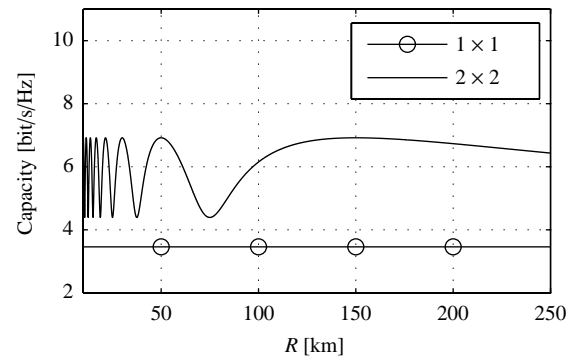


Figure 2 Capacity of a 2×2 system as a function of R when $\lambda = 0.3$ m ($f=1.0$ GHz), $d_t = 1500$ m, $d_r = 15$ m, $K \rightarrow \infty$, $\bar{\gamma} = 10$ dB, and $\theta_t = \theta_r = 0^\circ$.

In Fig.2, it is observed that the capacity indeed is maximized at $R_{opt} = 150\text{km}$, but it oscillates between two extremes for $R < R_{opt}$.⁶ The oscillation stems from ρ in (19), which for $n_R = 2$ is equal to $\rho = |\cos \frac{\pi}{2q}|$. Hence, for $R \leq R_{opt}$ ($\eta \leq 1$), it can be deduced that ρ is equal to

$$\rho = \begin{cases} 0 & \text{for } \eta = \frac{1}{(2q-1)} \\ 1 & \text{for } \eta = \frac{1}{2q} \end{cases}, \quad q \in \mathbb{Z}^+, q \neq 0. \quad (20)$$

At maximum capacity, the channel matrix is a full rank matrix ($r_\lambda = 2$) since the columns of the channel matrix are uncorrelated ($\rho = 0$). The capacity is then exactly twice the capacity of a 1×1 system. Denoting the distances where the channel matrix is full rank as $R_{\rho=0}$, it occurs at

$$R_{\rho=0} = \frac{2 \cos \theta_r \cos \theta_t d_t d_r}{(2q-1) \cdot \lambda}, \quad q \in \mathbb{Z}^+, q \neq 0. \quad (21)$$

At minimum capacity, the channel matrix is rank deficient ($r_\lambda = 1$) since the columns of the channel matrix are completely correlated ($\rho = 1$). Denoting the distances where the channel matrix is rank deficient as $R_{\rho=1}$, it occurs at

$$R_{\rho=1} = \frac{\cos \theta_r \cos \theta_t d_t d_r}{q \cdot \lambda}, \quad q \in \mathbb{Z}^+, q \neq 0. \quad (22)$$

In general, the distances related to a given correlation value between zero and one can be expressed as

$$R_\rho = \frac{\pi \cos \theta_r \cos \theta_t d_t d_r}{\lambda(\theta + \pi q)} = \frac{\pi}{2(\theta + \pi q)} R_{opt}, \quad (23)$$

where $q \in \mathbb{Z}^+$, $\rho = |\cos(\theta + \pi q)|$, and

$$\theta = \begin{cases} 0 < \theta < \frac{\pi}{2} & R > R_{opt} \\ \frac{\pi}{2} \leq \theta \leq \frac{3\pi}{2} & R \leq R_{opt} \end{cases}. \quad (24)$$

In Fig.3, the result of Fig.2 is reproduced but presented as function of both θ_r and R to visualize how the capacity varies with respect to range and misalignment between the ground and aircraft antenna. As such, Fig.3 can be viewed as an illustration of the capacity region covered by the ground antenna for an incoming aircraft at range R and angle θ_r relative to the ground antenna. It is assumed that $\theta_t = 0^\circ$. Once again, it is observed that the capacity fluctuates between two extremes given by either no correlation ($\rho = 0$) or complete correlation ($\rho = 1$). A relatively large area with a full rank matrix (white areas)

⁶A similar result is presented in [5, Fig. 2], but then as a function of d_t and d_r when R is fixed.

is observed in the area $100\text{km} \leq R \leq 250\text{km}$ and $-50^\circ \leq \theta_r \leq 50^\circ$. For distances closer than 100km , it is necessary to change the inter-element distance in the aircraft in order to exploit MIMO spatial multiplexing techniques, since the correlation between the subchannels of the channel matrix becomes too high (dark areas).⁷

An option is to mount more than two antennas at the aircraft and use a switch-based system to select the optimal two antennas for a given range and angle. Assuming that d_r is optimal (maximizes the capacity) at R_{opt} and $\theta_r = \theta_1$, the new optimal inter-element distance d_r^* at range R and $\theta_r = \theta_2$ is equal to

$$d_r^* = \frac{R \cos \theta_1}{R_{opt} \cos \theta_2} d_r. \quad (25)$$

By adjusting the inter-element distance close to d_r^* in a switch-based fashion as the aircraft closes in on the ground terminal, it is possible to stay in the vicinity

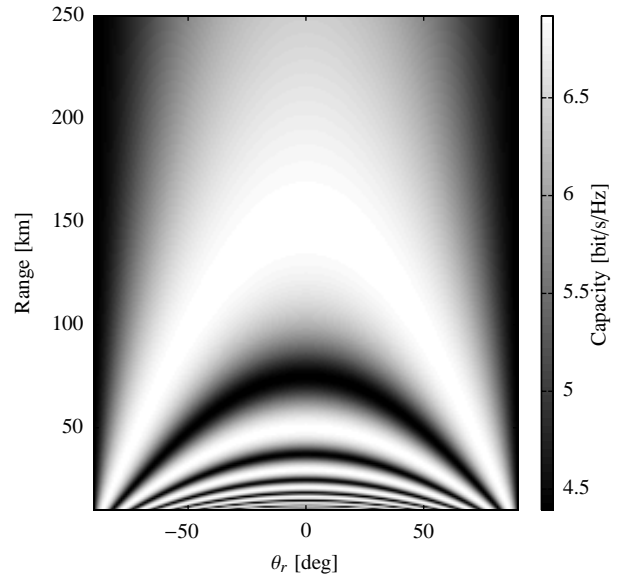


Figure 3 Capacity region of a 2×2 in a deterministic LOS channel ($K \rightarrow \infty$) as a function of θ_r and R .

⁷An additional ground terminal with a different coverage area could be used to give coverage for $\theta_r > \pm 50^\circ$ if antennas also could be placed along the fuselage of the aircraft. The combined coverage of two ground terminals will then ensure that θ_r in any case will be less than $\pm 50^\circ$.

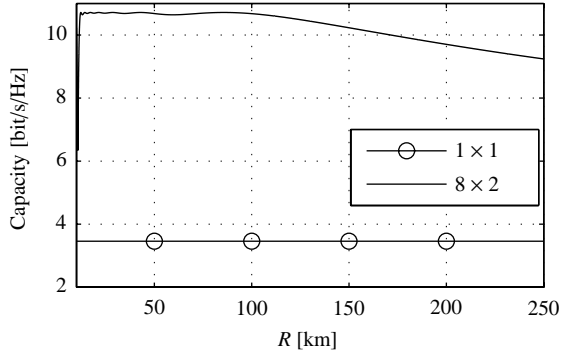


Figure 4 Capacity of a 8×2 system as a function of R when $\lambda = 0.3\text{m}$ ($f=1.0\text{GHz}$), $d_t = 1500\text{m}$, $d_r = 2.14\text{m}$, $K \rightarrow \infty$, $\bar{\gamma} = 10\text{dB}$, and $\theta_t = \theta_r = 0^\circ$.

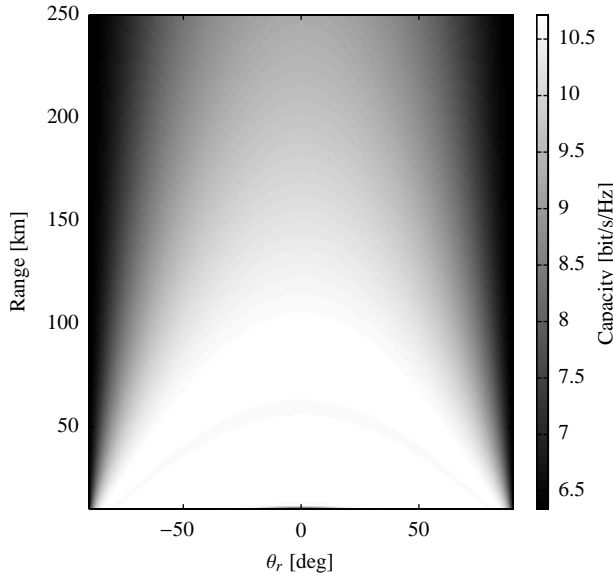


Figure 5 Capacity region of a 8×2 system in a deterministic LOS channel ($K \rightarrow \infty$) as a function of θ_r and R .

of the maximum of the capacity curve over an extended range. However, as the aircraft comes closer and closer to the ground terminal, the switching must be performed faster and faster to be in correlation with the fluctuation of the capacity curve. Hence, such an approach is not well suited when the aircraft comes at close range. A remedy to this challenge is explored in the next subsection.

4.1.2. $n_R \times 2$

A simple yet effective way to increase the robustness of the link in a strong LOS environment is simply to use more antennas at the receiver than at the transmitter and exploit all available antennas at the receiver at the same time rather than using a switched-based approach between a small subset of antennas.⁸ To illustrate this fact, Fig.4 shows the capacity of a 8×2 MIMO system. Compared to the 2×2 case, it is observed that the capacity has increased as a result of the increased number of antennas in the system. However, more importantly, the capacity curve does not contain the oscillations observed in the 2×2 system. Hence, the general condition $n_R > n_T$ has a stabilizing effect on the capacity curve as a function of range, and the effect resembles the stabilizing effect which antenna diversity has on the SNR level in a fading channel. Note that the receiver antenna length is assumed to be fixed at the reference length of 15m. Hence, in the 2×2 case, $d_t = 15\text{m}$, whereas in the 8×2 case, $d_t \approx 2.14\text{m}$. As a result of the increased number of antennas and the reduced inter-element distance, R_{opt} is reduced to approximately 86km in the 8×2 case compared to 150km in the 2×2 case.

In Fig.5, the capacity region of the 8×2 system is depicted. It clearly shows the improvement from the 2×2 case, as there are no fluctuations of the capacity curve in the entire range $10\text{km} \leq R \leq 250\text{km}$. The angle range is almost unchanged from the 2×2 case, i.e. $-50^\circ \leq \theta_r \leq 50^\circ$.

The increased stability of the capacity curve as a function of range can also be observed by examining the condition number $\kappa_{\mathbf{M}}$ of \mathbf{M} (and \mathbf{H}_{LOS}). The condition number is a measure of stability or sensitivity of a matrix (or the linear system it represents) to numerical operations, and matrices with a condition number close to one is said to be well-conditioned. The condition number of \mathbf{M} is equal to

$$\kappa_{\mathbf{M}} = \frac{\lambda_{\max}}{\lambda_{\min}} \triangleq \frac{n_R + |U_{n_R-1}(\cos x)|}{n_R - |U_{n_R-1}(\cos x)|} = \frac{1 + \rho}{1 - \rho}. \quad (26)$$

The condition number of \mathbf{H}_{LOS} may be obtained from $\kappa_{\mathbf{M}}$ by the following relation

$$\kappa_{\mathbf{M}} = \frac{\lambda_{\max}}{\lambda_{\min}} = \frac{\sigma_{\max}^2}{\sigma_{\min}^2} = \kappa_{\mathbf{H}_{\text{LOS}}}^2, \quad (27)$$

⁸The motivation for this particular approach comes from [7], where numerical results illustrate the relationship between the channel quality and the relative positions of a transmit and receiver node in a mm-wave MIMO architecture.

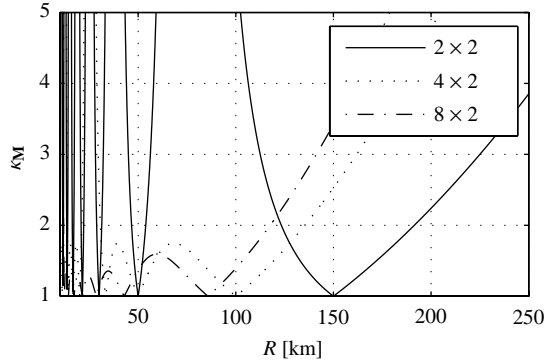


Figure 6 Condition number $\kappa_{\mathbf{M}}$ as a function of R and $n_R \in \{2, 4, 8\}$ with $\theta_t = \theta_r = 0^\circ$.

where σ_{\max} and σ_{\min} denote the maximum and minimum singular values of \mathbf{H}_{LOS} , respectively. Hence, when \mathbf{M} is well-conditioned, \mathbf{H}_{LOS} is well-conditioned. Using (15) and (16), the normalized correlation coefficient ρ can be expressed in terms of the condition number as

$$\rho = \frac{\kappa_{\mathbf{M}} - 1}{\kappa_{\mathbf{M}} + 1}. \quad (28)$$

From (28), it can be seen that a condition number close to one ensures that ρ is close to zero. In Fig.6, (26) is depicted as a function of n_R and R . It is observed that the range over which the condition number of \mathbf{M} (and hence \mathbf{H}_{LOS}) is close to one increases as n_R increases. Basically, this means that by increasing the number of receive antennas, \mathbf{H}_{LOS} may be kept at full rank over an extended range.

4.2. Part 2 - Stochastic channel

In this part, the capacity region results of the previous section obtained with the deterministic channel matrix \mathbf{H}_{LOS} are compared to simulation results obtained with the complete Rice fading channel matrix \mathbf{H} . Since \mathbf{H} is a stochastic matrix, the simulation results in this part are obtained by averaging over a number of channel realizations. According to [11], a typical Rice factor for the aeronautical channel in the en-route domain is $K = 15\text{dB}$. Hence, all the simulations are obtained for a Rice factor of $K = 15\text{dB}$. In Fig.7 and Fig.8, the capacity regions of a 2×2 and a 8×2 system are depicted, respectively. They both do not differ much from Fig.3 and Fig.5 obtained in a pure LOS channel.

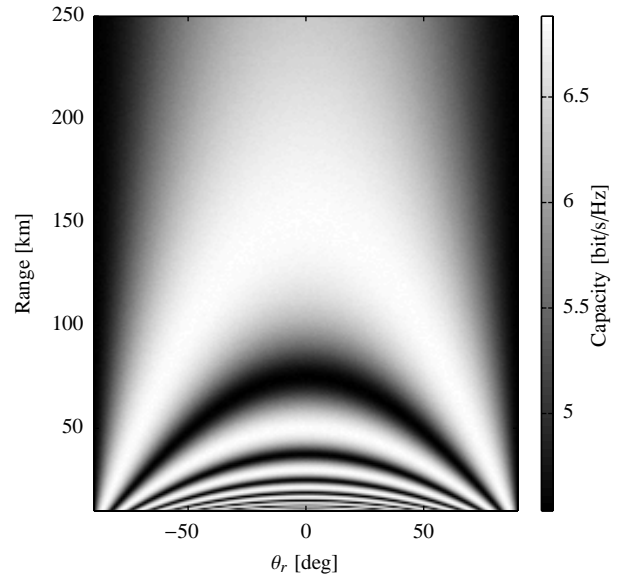


Figure 7 Capacity region of a 2×2 system in a Rice fading channel (averaged of 1000 channel realizations) as a function of θ_r and R with $\bar{\gamma} = 10\text{dB}$ and $K = 15\text{dB}$.

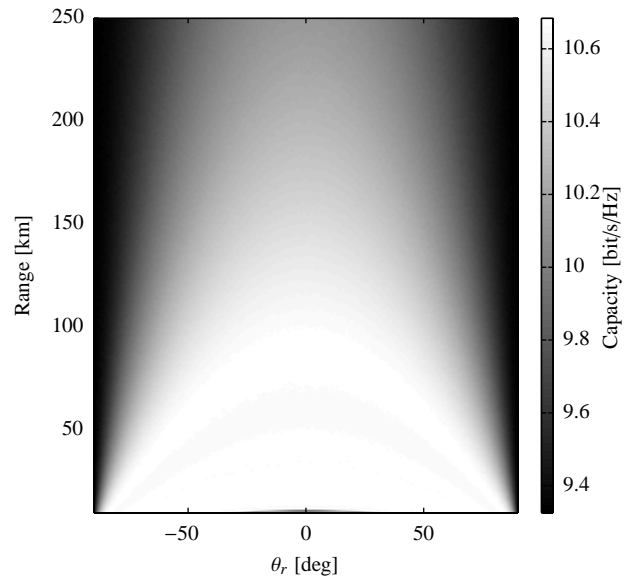


Figure 8 Capacity region of a 8×2 system in a Rice fading channel (averaged of 1000 channel realizations) as a function of θ_r and R with $\bar{\gamma} = 10\text{dB}$ and $K = 15\text{dB}$.

5. CONCLUSIONS

The results of this paper indicate that it is possible to exploit MIMO spatial multiplexing techniques in aeronautical communications over an extended range even in the presence of a strong LOS component. Numerical results are presented for a MIMO ground-to-air communication system with $n_T = 2$ transmit antennas (ground terminal) and an ULA antenna with $n_R \geq 2$ receive antennas (aircraft). The results show that a high rank channel matrix may be offered over an extended range (and area) when $n_R > n_T$, where the range improves as n_R increases. For an $n_R \times 2$ MIMO system with $n_R \geq 2$, the maximum number of spatial data pipes offered is two, and the n_R receive antennas contributes to stabilize the two data pipes in a LOS environment. Additional data pipes may be offered by increasing the number of transmit antennas but due to the large inter-element distance needed to obtain a large range, systems with more than two antennas in the ground terminal may not be very practical.

6. APPENDIX

Eigenvalues of \mathbf{M} for an $n_R \times 2$ MIMO system

For a $n_R \times 2$ system, using [4, Eq. (7)], the difference in path length from transmit antennas $l \in [0, 1]$ and $k \in [0, 1]$ to receive antenna $m \in [0, 1, \dots, n_R - 1]$ can be expressed as

$$\begin{aligned} r_{m,k} - r_{m,l} &= (l-k)d_t \sin \theta_t - (l^2 - k^2) \frac{(d_t \cos \theta_t)^2}{2R} \\ &+ \frac{d_t d_r \cos \theta_t \cos \theta_r}{R} (l-k)m \\ &= \alpha + \frac{d_t d_r \cos \theta_t \cos \theta_r}{R} (l-k)m, \end{aligned} \quad (29)$$

where $\alpha = (l-k)d_t \sin \theta_t - (l^2 - k^2) \frac{(d_t \cos \theta_t)^2}{2R}$. The channel matrix in (2) is simplified to

$$\mathbf{H} = \begin{bmatrix} h_{1,1} & h_{1,2} \\ h_{2,1} & h_{2,2} \\ \vdots & \vdots \\ h_{n_R,1} & h_{n_R,2} \end{bmatrix} \quad (30)$$

The individual terms of the matrix product $\mathbf{M} = \mathbf{H}_{\text{LOS}}^H \mathbf{H}_{\text{LOS}}$ can then be expressed as

$$\mathbf{M} = \begin{bmatrix} \mathbf{h}_0^H \mathbf{h}_0 & \mathbf{h}_0^H \mathbf{h}_1 \\ \mathbf{h}_1^H \mathbf{h}_0 & \mathbf{h}_1^H \mathbf{h}_1 \end{bmatrix}, \quad (31)$$

where

$$\mathbf{h}_0 = \left[e^{j\beta r_{0,0}}, \dots, e^{j\beta r_{n_R-1,0}} \right]^T, \quad (32)$$

$$\mathbf{h}_1 = \left[e^{j\beta r_{0,1}}, \dots, e^{j\beta r_{n_R-1,1}} \right]^T. \quad (33)$$

The inner product of the two channel vectors in (32) and (33) can in general be written as

$$\begin{aligned} \mathbf{h}_l^H \mathbf{h}_k &= \sum_{m=0}^{n_R-1} e^{j\beta(r_{m,k} - r_{m,l})} \\ &= \sum_{m=0}^{n_R-1} e^{j\beta \left(\alpha + \frac{d_t d_r \cos \theta_t \cos \theta_r}{R} (l-k)m \right)} \\ &= e^{j\beta \alpha} \cdot \sum_{m=0}^{n_R-1} e^{j \left(2\pi \frac{d_t d_r \cos \theta_t \cos \theta_r}{\lambda R} (l-k)m \right)} \\ &= e^{j\beta \alpha} \cdot \sum_{m=0}^{n_R-1} e^{jmu} \\ &= e^{j\beta \alpha} \cdot \frac{1 - e^{jn_R u}}{1 - e^{ju}} \\ &= e^{j\beta \alpha} e^{j(n_R-1)\frac{u}{2}} \cdot \frac{\sin\left(\frac{n_R u}{2}\right)}{\sin\left(\frac{u}{2}\right)} \\ &= e^{j\psi} \cdot \frac{\sin(n_R x)}{\sin x} \\ &= e^{j\psi} \cdot U_{n_R-1}(\cos x), \end{aligned} \quad (34)$$

where $u = 2\pi \frac{d_t d_r \cos \theta_t \cos \theta_r}{\lambda R} (l-k)$, $x = u/2 = \frac{\pi}{n_R \eta} (l-k)$, and $\psi = \beta \alpha + (n_R - 1)x$.⁹ Since $\mathbf{h}_0^H \mathbf{h}_1 = (\mathbf{h}_1^H \mathbf{h}_0)^*$, the matrix \mathbf{M} may be written compactly as

$$\mathbf{M} = \begin{bmatrix} n_R & e^{-j\psi} U_{n_R-1}(\cos x) \\ e^{j\psi} U_{n_R-1}(\cos x) & n_R \end{bmatrix}, \quad (35)$$

where $x = \frac{\pi}{n_R \eta}$.¹⁰ The eigenvalues of the matrix in (35) are derived from the characteristic equation, and they are equal to

$$\lambda_1 = n_R + U_{n_R-1}(\cos x), \quad (36)$$

$$\lambda_2 = n_R - U_{n_R-1}(\cos x). \quad (37)$$

7. ACKNOWLEDGEMENTS

This work has been funded by the Norwegian Research Council through the SECOMAS project (180018/S10).

⁹For the last equal sign in (34), see [16, Identity 4].

¹⁰In general, for an $n_R \times n_T$ system, x can be defined as $x = \frac{\pi}{n_R \eta} |l-k|$. The absolute value is introduced for simplicity since $\cos x = \cos(-x)$. Hence, if $(l-k) < 0$, $U_{n_R-1}(\cos(-x)) = U_{n_R-1}(\cos x)$.

8. COPYRIGHT

The authors confirm that they, and/or their company or institution, hold copyright of all original material included in their paper. They also confirm they have obtained permission, from the copyright holder of any third party material included in their paper, to publish it as part of their paper. The authors grant full permission for the publication and distribution of their paper as part of the EIWAC2010 proceedings or as individual off-prints from the proceedings.

9. REFERENCES

- [1] J. Rasool, G. E. Øien, J. E. Håkegård, and T. A. Myrvoll, "On multiuser MIMO capacity benefits in air-to-ground communication for air traffic management," in *Proc. 6th International Symposium on Wireless Communication Systems*, pp. 458–462, September 2009.
- [2] P. F. Driessen and G. J. Foschini, "On the capacity formula for multiple input-multiple output wireless channels: A geometric interpretation," *IEEE Transactions on Communications*, vol. 47, no. 2, pp. 173–176, February 1999.
- [3] D. Gesbert, H. Bölcskei, D. A. Gore, and A. J. Paulraj, "Outdoor MIMO wireless channels: Models and performance prediction," *IEEE Transactions on Communications*, vol. 50, no. 12, pp. 1926–1934, December 2002.
- [4] F. Bøhagen, P. Orten, and G. E. Øien, "Construction and capacity analysis of high-rank line-of-sight MIMO channels," in *Proc. IEEE Wireless Communications and Networking Conference*, vol. 1, pp. 432–437, March 2005.
- [5] I. Sarris and A. R. Nix, "Design and performance assessment of maximum capacity MIMO architectures in line-of-sight," in *Proc. IEE Commun*, vol. 153, no. 4, pp. 482–488, August 2006.
- [6] B. T. Walkenhorst and M. A. Ingram, "Repeater-assisted capacity enhancement (RACE) for MIMO links in a line-of-sight environment," in *Proc. IEEE International Conference on Communications*, pp. 1–6, June 2009.
- [7] E. Torkildson, C. Sheldon, U. Madhow, and M. Rodwell, "Millimeter-wave spatial multiplexing in an indoor environment," in *Proc. First International Workshop on Multi-Gigabit MM-Wave and Tera-Hz Wireless Systems*, November 2009.
- [8] M. Matthaiou, D. I. Laurenson, and C.-X. Wang, "Capacity study of vehicle-to-roadside MIMO channels with a line-of-sight component," in *Proc. IEEE Wireless Communications and Networking Conference*, pp. 775–779, April 2008.
- [9] E. Torkildson, C. Sheldon, U. Madhow, and M. Rodwell, "Nonuniform array design for robust millimeter-wave MIMO links," in *Proc. 28th IEEE Conference on Global Telecommunications*, pp. 4826–4832, December 2009.
- [10] F. Bøhagen, P. Orten, and G. E. Øien, "Design of optimal high-rank line-of-sight MIMO channels," *IEEE Transactions on Wireless Communications*, vol. 6, no. 4, pp. 1420–1425, April 2007.
- [11] E. Haas, "Aeronautical channel modeling," *IEEE Transactions on Vehicular Technology*, vol. 51, no. 2, pp. 254–264, 2002.
- [12] K. S. Gomadam and S. A. Jafar, "Modulation and detection for simple receivers in rapidly time varying channels," *IEEE Transactions on Communications*, vol. 55, no. 3, pp. 529–539, 2007.
- [13] D. Höslı and A. Lapidoth, "How good is an isotropic Gaussian input on a MIMO Ricean channel?" in *Proc. International Symposium on Information Theory*, p. 291, 2001.
- [14] B. Holter, "On the capacity of the MIMO channel: A tutorial introduction," in *Proc. IEEE Norwegian Symposium on Signal Processing*, pp. 167–172, 2001.
- [15] B. T. Walkenhorst, T. G. Pratt, and M. A. Ingram, "Improving MIMO capacity in a line-of-sight environment," in *Proc. IEEE Global Telecommunications Conference*, pp. 3623–3628, 2007.
- [16] A. T. Benjamin, L. Ericksen, P. Jayawant, and M. Shattuck, "Combinatorial trigonometry with Chebyshev polynomials," *Journal of Statistical Planning and Inference*, vol. 140, pp. 2157–2160, 2010.